In Silico Comparison of Main Proteinase Inhibitors for Different Coronaviruses

Tahani W. Jihad * 📧, *Hyffaa Y. Hussien* 📧 , *Mohammed A. M. Ali Qaba* 📧 , *Ghassan Q. Ismail* 📧

 Department of Chemistry, College of Science, University of Mosul, Mosul, Iraq.
*Corresponding author

Abstract

Coronaviruses are enclosed positive stranded RNA viruses with spike protein protrusions that permit the virus to penetrate and affect host cells. The emergence of Severe Acute Respiratory Syndrome Coronavirus (SARS-CoV) and Middle East Respiratory Syndrome Coronavirus (MERS-CoV), as mortal human CoV illnesses, has sparked considerable interest in the medical community. The fast and global outbreak of a novel human coronavirus generated by a novel progeny of coronavirus 2 (CoV-2) has promoted an urgent need to identify an effective target for COVID-19 treatment. The main proteinase MPro has been prominented as an appealing therapeutic target for coronaviruses, which is responsible for the transcriptase and replicase of coronaviruses. The identification of prospective medications is an imperative and critical need for the medical community. Molecular docking was used to describe the protease and asses the capacity of various well-known and laboratory-tested natural MPro inhibitors. Seventy-sixth natural compounds with known inhibitory activity and four medicines reported against CoV-1 were chosen for molecular docking study. Our in-silico studies reveal that many of these molecules show high binding affinity for several CoV-2 proteases and compare favorably to CoV-1 and MERS proteases. Our research indicates that these molecules could be anti CoV-2 MPro. implying their possibility for reprofiling as antiviral leads with broad scope .

Keywords: CoV-19, Cystine protease, Main proteinase, Molecular docking, Natural products.

Introduction

Coronaviruses are related to the family Coronaviridae, subfamily Coronavirinae, order Nidovirales, and are enclosed RNA viruses with a positive strand containing a helical protein shell, including genomes of 27–31 kb. They are categorised via four genera α, β, γ and δ. These viruses possess prominent spikes on their surface that give them structure like a crown, allowing them to bind to the respiratory systems and digestive tracts of birds and mammals, and they are restricted to one host species [1, 2].

Three coronaviruses have been documented worldwide. In 2002-2003, Guangdong, China identified a zoonotic incident delivered by civet cats and bats, resulting in severe acute respiratory syndrome (SARS). The SARS-CoV infection caused over 700 deaths. The pandemic was ended by using proper cleanliness and quarantine

measures[3, 4]. Another zoonotic transition involving camels was noted in 2012 in Saudi Arabia, resulting in infections of the lower respiratory tract in humans. 640 people died as a result of Middle East respiratory syndrome (MERS-CoV) [5, 6]. In 2019, a novel pandemic called novel coronavirus illness (nCoV) with symptoms similar to SARS was identified in China. SARS coronavirus 2 (SARS-CoV-2) has been distinguished to be the root of COVID-19, an outbreak of respiratory diseases in humans that results in acute pneumonia [7]. Despite numerous attempts and programs to contain the disease spread, it has spread rapidly throughout the world, with the related fatality rate increasing. According to the WHO, there have been over 1.6 million deaths. Because of the pathogen's novelty, no antiviral medicines or vaccines can lower the severity of the sickness or treat it. Furthermore, the acuteness of this virus has resulted in increased research on the sickness, resulting in a better perception of its aetiology, administration, and therapy [1].

SARS-CoV-2 is the seventh familiar coronavirus in humans, following NL63, 229E, HKU1 and OC43, SARS and MERS-CoV. The majority of human coronaviruses originated from bat covids and were transferred to humans *via* a moderator host [8].

The coronavirus genome is composed of 30,000 nucleotides which express non-structural proteins and structural proteins. 15 nonstructural proteins, a nucleocapsid protein that participates in synthesis of viral RNA, that encode NSP3 and NSP5 (main proteases), NSP12 (RNA polymerase-dependent RNA), NSP13 (triphosphatase/helicase), NSP14 (exoribonuclease), NSP15 (endonuclease) [9]. Four structural proteins, that comprises E (envelope), S (spike), M (membrane) and N (nucleocapsid) proteins profession during the entry into a host cell and virion formulation and release [10-12].

The main protease (M^{Pro} or NSP5), also called 3-Chymotrypsin-like protease (3CL^{Pro}), has a cleavage range similar to the 3C protease of picornavirus [13]. It is related to the cysteine protease group and cleaves polypeptides pp1ab at 11 locations with a sequence of Leu-Gln* (Ser, Ala, Gly) (*: cleavage site) [14, 15], a process started by the M^{Pro} auto-cleavage from polyproteins pp1a/pp1ab. This cleavage process corresponds to M^{Pro} in SARS-CoV [15-17]. In addition, the protease catalytic site includes a dyad of Cys145 and His41. The protease has three domains and the catalysis lies among domains I and

II [15, 18]. In the P2 domain of SARS-CoV polyproteins, there are three M^{Pro} cleavage sites include Met, Phe, or Val. Other coronaviruses, otherwise, lack similar cleavage sites. The Zhang group published the X-ray structure of the COVID-19 M^{Pro} complexed with a peptidomimetic α-ketoamide ligand at 1.95 Å. This research gave the first structural knowledge of the 3CL^{Pro} complexed SARS-CoV-2, which is a viable target for drugs to limit and inhibit infection of SARS-CoV-2 in patients [15].

Studies conducted recently have disclosed that chloroquine, hydroxychloroquine, ritonavir, lopinavir, remdesivir, azithromycin, dexamethansone, and ivermectin have the promise of inhibiting the severity of the disease in SARS-CoV-2 carriers [19-22]. Alternatively, numerous phytochemicals have been described in the literature to have potential antiviral action, which could be used as an alternative to limit coronavirus reproduction [23]. Natural molecules have a great chemical variety, a cheaper production cost than biotechnological compounds or outcomes synthesized by combinatorial chemistry, and have milder or no adverse effects than chemical medications [24].

In our study, after determining the crystal structure of M^{Pro}, we started searching for enzymes with a good identity ratio with this enzyme using FASTA alignment. We found two enzymes with a good identity ratio of 70 and 80%. These enzymes have been laboratory tested *in vitro* with some inhibitor classes that we chose to be studied theoretically with COVID-19 to find the best compounds and compared with other enzymes. In this context, the binding affinity of different inhibitor classes of phthalhydrazide-substituted ketoglutamine analogues, metal linked compounds, α, β-unsaturated peptidomimetics, aescin, anilides, isatin, aryl boronic acids, and other compounds were studied on the viral proteases binding sites from CoV-2, CoV-1 and MERS using molecular docking investigations and testing their molecular interaction and binding energy.

Materials and Methods

Modelling of Ligands

A library of 80 anti-SARS-CoV active inhibitors was created from scratch or based on reported X-ray structures for their locations. TL-3 and the known α-ketoamide ligands of SARS-CoV-2 M^{Pro} were obtained from their X-ray structures from protein data bank (https://www.rcsb.org) with PDB codes: 4K4P and 6Y2F. The remaining 78 inhibitors, were either sketched in 2D using ChemBioDraw Ultra 13 or retrieved from PubChem and saved in sdf format. MOE was also used to convert their 2D structures to 3D structures and to minimise them. The tested inhibitors and complexed ligands were then transferred to a certain database and stored as a mdp file in preparation for use in the coronavirus docking investigation. MMFF: Amber 10 force field was employed to optimize the designed structures.

Preparation of Viral Proteases

The crystal structures were created using the detailed technique outlined previously [25, 26]. The crystal structures of SRAS-CoV-2 M^{Pro}, SARS-CoV M^{Pro} and MERS-Cov CL^{Pro} were obtained from the PDB Database (https://www.rcsb.org). PDB codes: 6Y2F, 6LU7, 6WTT, 7C8U, 7CA8 and 7JQ2 for CoV-2, 1UK4 and 3C3N for CoV-1, 4RSP for MERS-CoV with resolutions of 1.95, 2.16, 2.15, 2.35, 2.45, 1.40, 2.50, 2.20 and 1.62 Å respectively. A typical structure of PDB may contain metal ions, water molecules, co-crystallised ligands and cofactors. In addition, multimeric structures may require a reduction to one unit. All water molecules were removed except that existed in active site if existed, and all structures were preprepared for docking with the MOE module (Molecular Operating Environment) (http://www.chemcomp.com), which adds protons to structures where protons were absent and sets the force field at pH 7.0. Subsequently, the ligands complexed with these enzymes were chosen to create a radius sphere of 4.5 Å, which was dubbed the ligand binding site.

Molecular Docking Investigations of Anti-SARS-CoV Inhibitors with Main Protease Targets

Molecular docking investigations of prepared anti-SARS-CoV inhibitors on the active places of prepared SARS-CoV-2 M^{Pro}, SARS-CoV M^{Pro} and MERS-CoV CL^{Pro} were performed using the MOE software (Molecular Operating Environment) (http://www.chemcomp.com). To find a potent inhibitor with potential enzyme-inhibitory properties for treating CoV-2, we selected M^{pro} as a target enzyme. The chemical compositions of natural compounds and drugs employed in the docking study are shown in Fig. 1. To apply charges and parameters, the MMFF94x force field was used. After creating and isolating the active site with MOEs surface and mapping module, the ligands were docked on the inside surface of the target receptor employing the Dock module of MOE. To perform docking studies, triangle matcher and refinement approaches were used. For each trialed ligand, the rigid receptor was used as the refining protocol and the GBVI/WSA dG as the scoring protocol to choose the best pose from 100 varied poses. The active site was used as ligand atoms, and automatic rotational bonds were permitted. To their default rates, the scoring methodologies were adopted. After the docking processes were completed, the poses acquired were analysed, and the top ones with the best suited docking score values in the active site were picked.
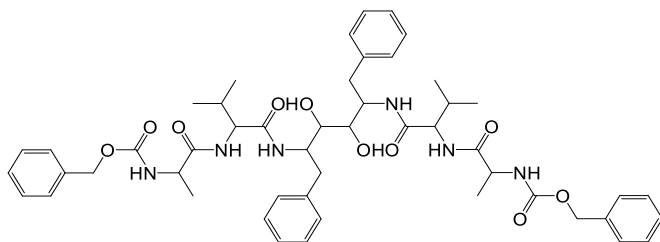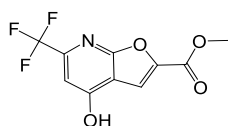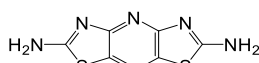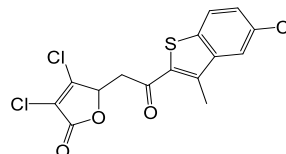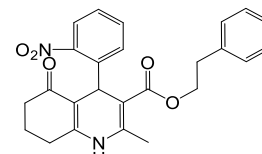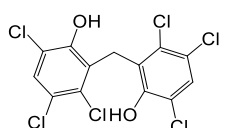
3TL (1)
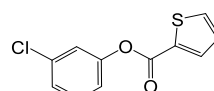
MAC-5576 (2)
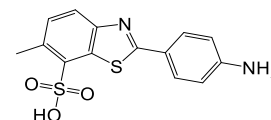
MAC-8120 (3)

MAC-13985 (4)

MAC-22272 (5)

MAC-30731 (6)

MP 576 (7)

Hexachlorophene (8)
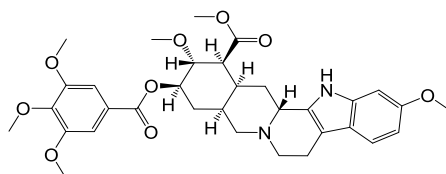
Reserpine (9)
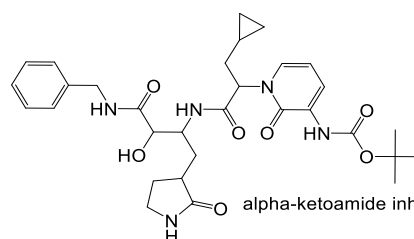
alpha-ketoamide inhibitor (10)
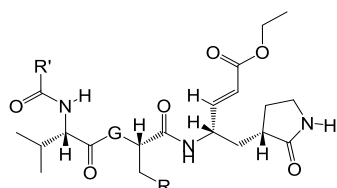
AG7088 (11-14), G=CH₂ AG7088 (15-18), G=NH
11, 15: R=4-F-C₆H₄, R'= 5-Methyl-3-isoxazole
12, 16: R=4-F-C₆H₄, R'= PhCH₂O
13, 17: R=Ph, R'= 5-Methyl-3-isoxazole
14, 18: R=Ph, R'= PhCH₂O
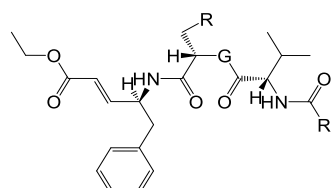
AG7088 (19-22), G=CH₂ AG7088 (23-26), G=NH
19, 23: R=4-F-C₆H₄, R'= 5-Methyl-3-isoxazole
20, 24: R=4-F-C₆H₄, R'= PhCH₂O
21, 25: R=Ph, R'= 5-Methyl-3-isoxazole
22, 26: R=Ph, R'= PhCH₂O
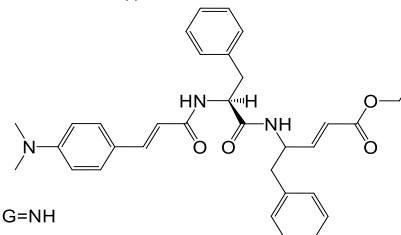
unsaturated ester (27)
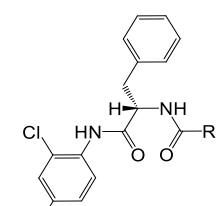
Anilide (28-34)
28: R=t-BuO
29: R=Me₂NC₆H₄
30: R= C₁₄H₂₉CH(Br)
31: R= 3,4-(NH₂)₂C₆H₃
32: R= (Indol-3-yl)-CH-=CH
33: R= (2-NH₂-1,3-thiazol-4-yl)-C(=NOCH₃)
34: R=Et₂NC₆H₄
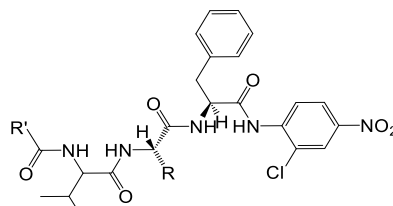
Tripeptide anilide (35-41)
35: R= i-Bu, R'= Et
36: R= i-Bu, R'= Ph
37: R= i-Bu, R'= t-BuO
38: R= i-Bu, R'= morpholino
39: R= i-Bu, R'= Thien-2-yl
40: R= PhCH₂, R'= Thien-2-yl
41: R= PhCH₂, R'= 5-Me-isoxazol-3-yl
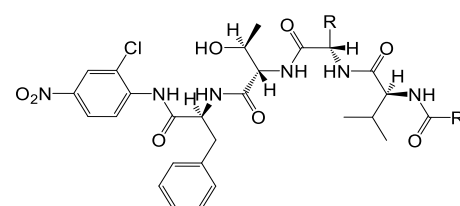
Tetrapeptide anilide (42-48)
42: R=i-Bu, R'=Et
43: R=i-Bu, R'=morpholino
44: R=PhCH₂, R'=t-Bu
45: R=PhCH₂, R'= 5-Me-isoxazole-3-yl
46: R=PhCH₂, R'= PhCH₂O
47: R= 4-FC₆H₄CH₂, R'= Et
48: R= 4-FC₆H₄CH₂, R'= Ph
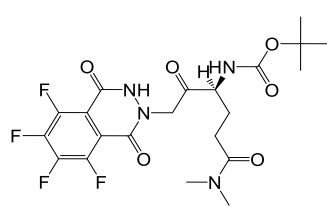
N,N-Dimethylglutamine (49)
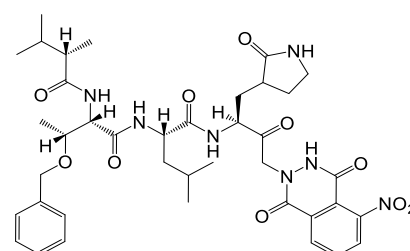
Keto-glutamine (50)
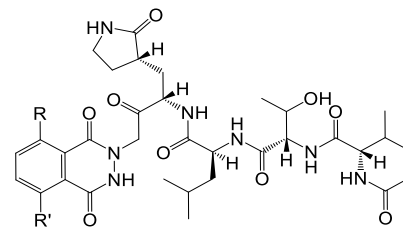
Glutamine (51-52)
51: R=R'=H
52: R= H, R'=NO₂
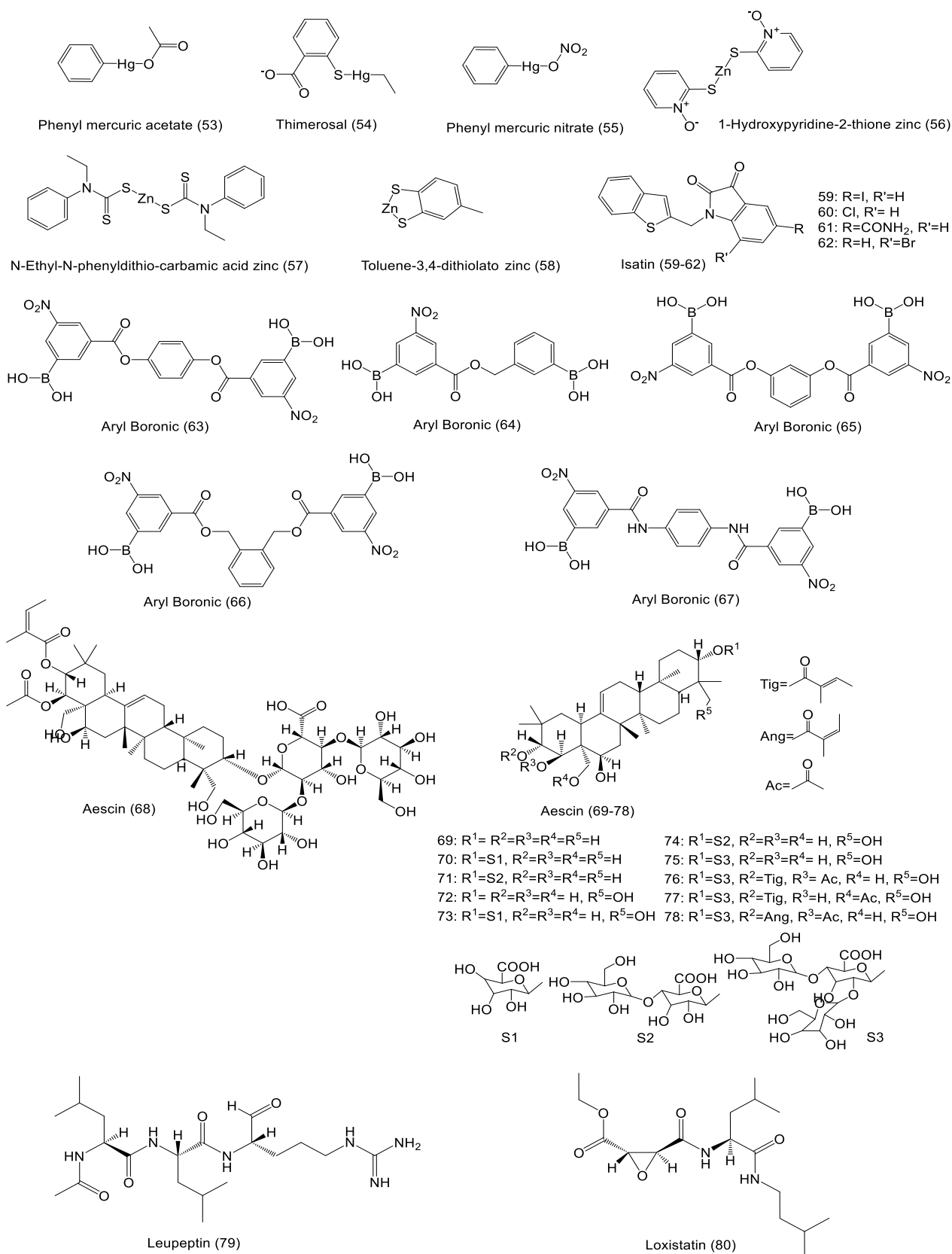
Figure 1. Chemical compositions of natural compounds and drugs tested against M^{Pro} of SARS and MERS-CoV

Results and discussion

Molecular docking or other computer-aided techniques are effective tools for studying the molecular features of bindings between protein and ligand through drug development for a number of previously prominent and lethal diseases, involving the coronavirus (SARS) [27-29]. In this research, MOE software was used to conduct a computational analysis of many natural products against coronavirus target main proteases in order to discover the top hits from each family among 80 compounds, depending on their docking scores. The superior-ranked compounds had higher negative docking score rates and higher M^{Pro} linking affinities. Consequently, in two stages, twelve hits that could potentially be CoV-2 M^{Pro} inhibitors were identified. First, a doc was run on all enzymes with PDB codes: 6Y2F, 6LU7, 6WTT, 7C8U, 7CA8 and 7JQ2 for CoV-2, 1UK4 and 3C3N for CoV-1, 4RSP for MERS-CoV for compounds known as CoV-1 and MERS inhibitors, and 790 compounds emerged as the best pose for each compound with the enzymes already indicated Table 1.

In the second stage, we selected the best docking score related to each family of compounds with CoV-2 and compared it to CoV-1 and MERS Table 2. The docking investigation of chosen compounds to M^{Pro} of COVID19 yielded binding affinities ranging from -6.53 to -9.80 kcal/mol, which were compared to CoV-1 and MERS docking scores Table 2. These compounds include the top scores of TL-3, reserpine, $\alpha$-ketoamide, leupeptin, loxistatin, and other inhibitors from each class listed in Table 1. Compounds 7, 46, 79 and 80 were found to have docking score values against CoV-2 lower than CoV-1 but higher than MERS, whereas compound 46 had the top linking affinity to those viral proteases. As a result, compound 46 was the tightest docked molecule to M^{Pro} that embedded the coronavirus target protein. Compound 12 was in the second place in the list, docking at -9.57, with CoV-2 $3CL^{Pro}$, a docking score surpassing CoV-1 and MERS. Compounds 9, 10, 50, 62, 66 and 78 followed a similar pattern. The TL-3 ranked third against CoV-2, with a docking score of -9.48 kcal/mol, compared to -8.24 kcal/mol for CoV-1 and -9.60 kcal/mol for MERS $3CL^{Pro}$. The interactions of the best inhibitors with amino acid units of $3CL^{Pro}$ of CoV-2 Table 3 revealed that these molecules mostly engaged with the units *via* H-bonding and hydrophobic effects. The outcomes of the finest molecular docking inhibitors in the $3CL^{Pro}$

active site of CoV-2 are shown by their individual 2D interaction graphs discovered by MOE Fig. 2. These findings clearly reveal that each of the molecules binds to the proteases active sites and hence may be predicted to decrease enzyme activity and thus limit viral multiplication.

Furthermore, ADME-Toxicity investigated the physiochemical features of these ligands using the filter Lipinski's rule of 5 criteria for determining drug identity. The molecular features that are significant for a drug pharmacokinetics within a human body are established by Lipinski's rule. Lipinski's five criteria for a typical drug 1) a molecular mass of fewer than 500 g/mol, 2) no more than 5 hydrogen-bond donors, 3) no more than 10 hydrogen-bond acceptors, 4) a partition factor (log P) for octanol/water not larger than 5. Violations of three or more of the criteria does not meet drug-likeness criteria when administered through the oral track [30]. Based on physiochemical features of the top twelve docked ligands and by matching to Lipinski's criteria, we concluded nine compounds fit totally and three others partially for containing violations Table 4.

As a result, computational investigations resulted in the identification of certain molecules as possible inhibitors of M^{Pro} of CoV-2, which demonstrated the top binding scores and affinities. Furthermore, our computational studies reveal that these substances could prohibit other viral proteases as SARS-CoV-1 $3CL^{Pro}$ and MERS-CoV CL^{Pro}, and by comparing the results, we can assume that molecules with higher docking scores than CoV-1 and/or MERS may show higher inhibitory activity than SARS-CoV-1 and MERS at lower concentrations when tested in the lab, and thus could be developed into potential pharmaceutical candidates for COVID-19.

Table 1. Details of the adopted natural compounds and drugs docking scores to COVID proteases, 6Y2F, 6LU7, 6WTT, 7C8U, 7CA8, 7JQ2, 1UK4, 3C3N and 4RSP. Also, considering their activity against SARS-CoV.

Groups of ligands	No	CoV-2						CoV-1	MERS-CoV		Ki^a or IC_{50}^b (μM)	Ref.
		6y2f	6lu7	6wtt	7c8u	7ca8	7jq2	1uk4	3c3n	4rsp		
						Dock scores kcal/mol						
TL-3	1	-9.48504	-9.04559	-9.33968	-8.82893	-8.33498	-9.27313	-8.24804	-7.95373	-9.60045	0.6[a]	[31]
Miscellaneous	2	-5.0979	-5.37147	-5.39782	-5.28356	-5.18322	-5.37521	-4.81399	-6.16008	-5.43814	0.5[b]	[32]
	3	-5.91951	-6.37405	-6.10158	-6.24328	-5.94081	-6.48196	-5.40074	-6.30766	-6.65522	4.3[b]	[32]
	4	-5.08948	-4.99913	-4.82489	-5.14095	-4.53851	-5.10686	-4.44997	-5.51888	-4.90053	7[b]	[32]
	5	-4.63987	-4.78117	-4.71457	-4.79674	-4.40197	-5.00187	-4.85857	-5.35186	-4.87774	2.6[b]	[32]
	6	-5.99018	-5.902	-5.947	-6.07561	-5.49927	-6.13447	-5.40555	-7.37683	-6.25658	7[b]	[32]
	7	-6.44857	-6.80545	-6.70784	-6.9877	-6.35221	-6.81777	-6.1703	-8.27766	-6.91454	2.5[b]	[33]
	8	-5.7129	-5.97953	-6.01441	-5.77354	-5.99967	-5.64899	-4.94684	-6.40736	-6.09905	13.7[a]	[34]
Reserpine	9	-7.74008	-7.88282	-7.58358	-7.36877	-6.7703	-7.36447	-6.79652	-7.33656	-7.49394	3.4[b]	[31]
α-Keto amide	10	-7.92988	-8.1746	-8.2285	-8.61301	-7.20986	-8.97155	-7.15213	-6.68094	-8.4924	0.67[b]	[15]
α, β-Unsaturated ester	11	-7.96728	-8.37465	-7.91003	-8.4967	-7.51142	-8.20956	-6.86082	-8.1981	-8.60288	>100[b]	[35]
	12	-8.47361	-9.07683	-9.57232	-8.69457	-7.62091	-8.3374	-7.41789	-7.48223	-9.45058	>100[b]	[35]
	13	-8.99802	-8.12875	-8.24664	-8.33036	-7.41102	-8.06207	-6.97778	-7.68585	-9.18952	>100[b]	[35]
	14	-8.6962	-8.6758	-8.1628	-8.0738	-7.5995	-8.5884	-7.339	-7.737	-9.0575	>100[b]	[35]

		3	6	2	9	1	2	91	99	6		
	15	-8.81642	-8.43631	-8.34132	-8.02333	-7.49714	-8.45909	-7.44278	-8.13821	-8.65589	>100[b]	[35]
	16	-8.25708	-8.69742	-8.47438	-8.48437	-7.79844	-8.41952	-7.06331	-8.30234	-9.12342	>100[b]	[35]
	17	-8.67642	-9.00436	-9.1454	-8.13641	-7.94752	-8.43995	-7.31932	-7.65704	-8.89465	80[b]	[35]
	18	-8.89064	-8.3436	-8.29996	-8.75958	-7.36858	-8.53162	-7.47841	-7.37075	-8.72465	85[b]	[35]
	19	-7.62959	-8.19528	-8.21516	-8.07221	-7.95887	-8.06423	-7.36283	-8.76326	-8.79728	39[b]	[35]
	20	-8.15564	-9.04244	-8.9996	-8.38311	-7.97506	-8.81959	-7.6014	-7.50571	-10.0443	31[b]	[35]
	21	-8.70733	-8.37615	-8.29999	-8.64983	-7.7915	-8.28956	-7.35129	-7.3952	-8.56816	13[b]	[35]
	22	-8.44288	-9.02199	-8.59027	-8.45331	-7.76474	-8.67385	-7.66199	-8.31188	-8.9156	38[b]	[35]
	23	-8.04325	-8.30649	-8.48699	-8.06935	-7.44697	-8.60181	-7.51633	-8.12271	-8.46556	21[b]	[35]
	24	-8.31477	-9.00493	-8.56803	-8.19214	-8.06413	-9.29912	-7.16575	-8.63962	-8.98067	11[b]	[35]
	25	-8.48505	-8.28026	-8.01052	-8.34395	-7.46856	-8.22915	-6.94893	-8.11548	-8.33251	30[b]	[35]
	26	-8.41993	-8.0283	-9.37681	-8.50295	-8.12239	-9.1264	-7.44049	-7.68198	-9.69467	11[b]	[35]
	27	-8.01424	-7.98006	-8.07257	-8.33112	-7.72831	-9.08958	-7.4683	-7.75536	-8.56755	0.5[a]	[35]
Anilide	28	-6.93693	-7.25716	-7.14419	-7.1654	-6.4637	-7.65667	-6.81121	-7.5588	-7.57829	>50[b]	[36]
	29	-6.84806	-7.38948	-6.9526	-7.17293	-7.24009	-7.89476	-6.40625	-7.90869	-7.41175	0.06[b]	[36]
	30	-7.97551	-7.928	-7.93493	-7.7809	-8.04548	-8.46524	-7.29429	-8.99697	-8.20436	3[b]	[36]
	31	-7.19014	-7.57145	-7.03796	-7.05938	-7.2656	-7.4039	-6.27625	-8.00734	-7.53302	2[b]	[36]
	32	-7.1731	-7.49444	-7.25121	-7.33797	-7.07178	-7.73189	-6.44824	-8.83422	-7.54181	3[b]	[36]
	33	-7.29586	-7.65959	-7.57525	-7.65025	-7.80351	-7.85309	-6.5272	-7.68614	-7.68607	7[b]	[36]

	No										Value	Ref
Tripeptide anilide	34	-7.20914	-7.17337	-7.01861	-7.45565	-6.88715	-7.29924	-6.37821	-8.50928	-7.51824	0.03[a]	36
	35	-8.35434	-8.41452	-8.85089	-8.41664	-7.12471	-8.16804	-6.85845	-8.78553	-8.7041	7[b]	36
	36	-8.24942	-8.74485	-8.63409	-8.28518	-8.08964	-9.07999	-7.40694	-9.06039	-9.53301	4[b]	36
	37	-8.25369	-8.35374	-8.58784	-7.906	-7.51081	-8.28034	-7.32895	-9.87628	-8.68305	>10[b]	36
	38	-8.65608	-9.44862	-8.51925	-8.07206	-8.08289	-8.55919	-7.27396	-8.20199	-8.86371	19[b]	36
	39	-8.69307	-8.7875	-9	-8.08909	-8.00853	-8.86913	-7.49059	-8.20744	-8.68811	5[b]	36
	40	-8.42869	-8.39907	-8.59991	-8.68591	-8.11009	-8.64441	-7.46218	-8.58431	-9.18289	5[b]	36
Tetrapeptide anilide	41	-8.25686	-8.12471	-7.81966	-8.05263	-8.36868	-8.22484	-7.05	-8.69019	-8.40879	7[b]	36
	42	-8.57779	-8.5467	-8.73503	-8.34821	-7.54819	-8.58917	-8.04949	-9.07849	-9.32647	7[b]	36
	43	-8.49401	-8.66311	-8.38143	-8.72641	-8.31909	-9.13441	-7.83077	-8.66435	-8.99721	16[b]	36
	44	-8.85332	-9.03422	-9.27931	-8.52784	-8.4111	-9.5844	-7.68642	-8.50307	-9.00092	2[b]	36
	45	-8.57383	-8.44681	-9.29522	-8.71522	-7.80902	-9.77617	-7.70102	-9.73331	-8.94105	5[b]	36
	46	-9.80851	-9.02552	-9.22656	-8.84297	-8.18922	-8.47119	-7.6283	-10.30886	-9.70139	6[b]	36
	47	-8.84545	-8.04963	-8.71293	-8.80225	-7.91696	-9.71409	-8.0958	-9.01385	-8.83314	5[b]	36
	48	-8.46823	-9.13453	-8.41206	-8.85143	-8.11665	-8.38551	-7.70804	-8.70027	-9.79704	2[b]	36
Keto-glutamine analogue	49	-6.98453	-7.12915	-6.73764	-7.19366	-6.19036	-7.4876	-6.56506	-7.52378	-7.72137	9±2[a]	37
	50	-8.75195	-8.33057	-9.27131	-9.40438	-7.77932	-7.95644	-7.58115	-8.42451	-9.38211	0.6[b]	37
	51	-8.5388	-8.3308	-8.8192	-8.2296	-7.7978	-8.3521	-7.485	-8.716	-9.8401	2.9[b]	37

Group	No.										Value	Ref
		6	6	2	9	7	2	76	66	8		
Metal-conjugated	52	-8.4515	-8.6342	-8.52757	-8.79885	-7.7377	-9.25328	-5.57687	-7.94973	-9.53577	3.4[b]	37
	53	-4.39194	-4.4726	-4.27204	-4.38414	-4.26446	-4.36029	-4.11938	-4.67712	-4.47441	0.7[a]	34
	54										2.4[a]	34
	55	-4.07687	-4.27233	-4.1948	-4.0911	-3.85804	-4.21436	-3.94735	-4.29484	-4.34544	0.3[a]	34
	56	-5.43634	-5.74266	-5.57486	-5.5968	-5.55108	-5.62579	-5.08932	-6.75317	-5.64164	0.17[a]	34
	57	-6.40804	-6.28136	-6.49303	-6.29674	-6.24286	-6.25426	-5.82071	-7.02101	-6.20839	1.0[a]	34
	58	-4.29278	-4.48497	-4.35032	-4.44091	-4.60672	-4.45695	-3.90363	-4.88346	-4.39116	1.4[a]	34
Isatin	59	-5.8688	-5.53436	-6.02438	-5.81962	-5.15652	-5.75266	-5.28718	-6.05447	-5.96115	0.95[b]	38
	60	-5.93186	-5.54326	-6.03102	-5.82186	-5.49507	-5.74933	-5.286	-6.0528	-5.96676	0.9[b]	38
	61	-6.37891	-5.80689	-6.12908	-6.26161	-5.81666	-5.91915	-5.48993	-6.6748	-6.33658	0.002[b]	38
	62	-5.77878	-6.53619	-6.1972	-5.84337	-5.87825	-6.09145	-5.03029	-5.74218	-6.06743	0.98[b]	38
Aryl Boronic Compounds	63	-7.73895	-8.14708	-7.85617	-7.29446	-7.42513	-7.57044	-7.28138	-8.66107	-7.8019	4.5[a]	39
	64	-7.15681	-7.48248	-7.80872	-7.55086	-7.08086	-7.41637	-6.76019	-8.78592	-7.62294	16[a]	39
	65	-7.69664	-7.9093	-8.12658	-7.93161	-7.47214	-8.13046	-7.53214	-8.9809	-8.45218	6[a]	39
	66	-8.92199	-8.22738	-8.60609	-8.44373	-7.79513	-8.25054	-7.81488	-8.69716	-8.82574	6[a]	39
	67	-7.26627	-7.53629	-7.30204	-7.08643	-7.04243	-7.70593	-6.95418	-7.78984	-7.3308	0.04[a]	39
Aescin	68	-7.94944	-8.18594	-7.47463	-7.39725	-7.03783	-6.99506	-7.67173	-6.42242	-7.47297	6.0[b]	31
	69		-5.28487									40
	70	-	-	-	-	-	-	-	-	-		40

Compound	Cpd. No											Ref
		6.60235	6.67751	6.30988	6.46494	5.91104	5.92234	6.04475	3.95553	6.33804		
	71	-6.84318	-7.4057	-6.91001	-6.92251	-6.00403	-6.76062	-6.67663	-6.69071	-7.9121		40
	72	-3.69181	5.01259	4.98501	4.5686	4.25871	3.0931					40
	73											40
	74								-4.80784			40
	75	-8.15099	-7.89442	-7.39303	-7.72792	-6.84101	-7.05733	-7.23708	-5.16369	-7.51789		40
	76	-8.32518	-8.14388	-7.12785	-7.188	-6.70662	-7.56005	-7.08449	-3.46448	-7.00871		40
	77		-7.46005	5.5438		5.31772		-6.44877	-1.07241			40
	78	-8.42585	-8.14202	-7.58415	-7.04908	-6.58184	-7.14486	-7.49793	4.79542	-7.58374		40
Leupeptin	79	-7.21173	8.04749	-7.65786	7.9912	-7.04795	7.82826	-6.55891	8.3242	-7.5992	127.2 b	41
Loxistatin	80	-7.09766	7.57659	-7.30901	6.98791	6.6406	7.4564	-5.76298	8.7296	7.13249		

Table 2. The natural compounds and drugs docking scores with 3CL^{Pro} of coronaviruses (PDB code=6Y2F, 6LU7, 6WTT, 7C8U, 7CA8, 7JQ2, 1UK4, 3C3N and 4RSP)

Cpd. No.	Compound Name	Binding affinity		
		CoV-2	CoV-1	MERS-CoV
46	Tetrapeptide anilide	-9.80/6Y2F	-10.30/3C3N	-9.70/4RSP
12	α, β-Unsaturated ester	-9.57/6WTT	-7.48/3C3N	-9.45/4RSP
1	TL-3	-9.48/6Y2F	-8.24/1UK4	-9.60/4RSP
50	Ketoglutamine	-9.40/7C8U	-8.42/3C3N	-9.38/4RSP
10	α-ketoamide	-8.97/7JQ2	-7.15/1UK4	-8.49/4RSP
66	Aryl Boronic	-8.92/6Y2F	-8.69/3C3N	-8.82/4RSP
78	Aescin	-8.42/6Y2F	-7.49/1UK4	-7.58/4RSP
79	Leupeptin	-8.04/6LU7	-8.32/3C3N	-7.59/4RSP
9	Reserpine	-7.88/6LU7	-7.33/1UK4	-7.49/4RSP
80	Loxistatin	-7.57/6LU7	-8.72/3C3N	-7.13/4RSP
7	MP576	-6.98/7C8U	-8.27/3C3N	-6.91/4RSP
62	Isatin	-6.53/6LU7	-5.74/3C3N	-6.06/4RSP

Table 3. Interaction of natural molecules and drugs with amino acid units of 3CL^{Pro} of coronaviruses (*PDB code)

Cpd. No.	Binding Affinity CoV-2	Ligand	Receptor	Interaction	Distance	E (kcal/mol)
46	-9.80/6Y2F*	O 44	N GLY 143 (A)	H-acceptor	3.04	-2.0
		6-ring	NE2 HIS 163 (A)	pi-H	4.69	-1.0
12	-9.57/6WTT*	N 68	OE1 GLN 189 (A)	H-donor	2.91	-2.4
		O 86	N GLU 166 (A)	H-acceptor	2.95	-4.1
1	-9.48/6Y2F*	O 23	N GLU 166 (A)	H-acceptor	3.54	-0.6
		C 34	5-ring HIS 41 (A)	H-pi	3.71	-0.6
		6-ring	CA THR 24 (A)	pi-H	4.35	-0.8
		6-ring	CG2 THR 24 (A)	pi-H	4.55	-0.6
		6-ring	NE2 GLN 189 (A)	pi-H	4.27	-0.7
50	-9.40/7C8U*	O 87	N GLU 166 (A)	H-acceptor	3.12	-3.2
		O 102	OG SER 144 (A)	H-acceptor	2.93	-1.0
10	-8.97/7JQ2*	N 3	SG CYS 145 (A)	H-donor	3.56	-3.3
		C 20	O GLU 166 (A)	H-donor	3.28	-1.1
		O 39	N GLU 166 (A)	H-acceptor	2.89	-2.6
66	-8.92/6Y2F*	O 36	N GLY 143 (A)	H-acceptor	2.96	-2.4
		O 39	N GLU 166 (A)	H-acceptor	3.16	-3.1
		O 48	GLN 192 (A)	H-acceptor	3.10	-2.6
78	-8.42/6Y2F*	O 12	O THR 24 (A)	H-donor	3.04	-1.2
		O 63	OD1 ASN 142 (A)	H-donor	2.83	-1.7
		O 67	SG CYS 145 (A)	H-donor	3.59	-0.8
79	-8.04/6LU7*	N 26	SG CYS 145 (A)	H-donor	4.36	-1.7
		N 45	OE1 GLN 189 (A)	H-donor	2.82	-0.8
		N 61	O PHE 140 (A)	H-donor	3.06	-2.0
		O 23	N SER 144 (A)	H-acceptor	2.95	-1.4
9	-7.88/6LU7*	C 5	OE1 GLN 189 (A)	H-donor	3.27	-0.9
80	-7.57/6LU7*	N 18	SG CYS 145 (A)	H-donor	4.00	-2.4
		O 10	NE2 HIS 163 (A)	H-acceptor	2.94	-4.5
		C 42	5-ring HIS 41 (A)	H-pi	3.81	-0.6
7	-6.98/7C8U*	O 43	N GLU 166 (A)	H-acceptor	3.13	-0.9
		6-ring	CB ASN 142 (A)	pi-H	4.01	-0.9
62	-6.53/6LU7*	O 32	OG SER 144 (A)	H-acceptor	2.94	-1.3
		5-ring	CA ASN 142 (A)	pi-H	4.13	-0.6

Table 4. Physiochemical evaluation of twelve natural compounds as effectual SARS-CoV-2 3CL^{Pro} inhibitors

| Cpd. No.	Lip-druglike	weight	logP(o/w)	ASA	a-acc	a-don	violation
46	0.0	801.2970	5.6580	1147.1008	6.0	6.0	3
12	1.0	623.7220	4.2740	1021.0816	5.0	3.0	1
1	0.0	909.0940	6.0920	1276.1167	8.0	8.0	3
50	0.0	777.8760	3.2750	1059.6309	8.0	5.0	2
10	0.0	595.6970	1.5720	923.0005	6.0	5.0	2
66	0.0	524.0100	3.4840	808.8318	6.0	4.0	2
78	0.0	1131.2689	-1.7775	1362.2352	22.0	14.0	4
79	1.0	426.5620	1.6270	784.4965	5.0	6.0	0
9	0.0	608.6880	3.6812	946.0501	8.0	1.0	2
80	1.0	342.4360	2.0930	678.4503	4.0	2.0	0
7	1.0	432.4760	4.3740	688,0418	2.0	1.0	0
62	1.0	372.2420	4.2260	512.9424	2.0	0.0	1
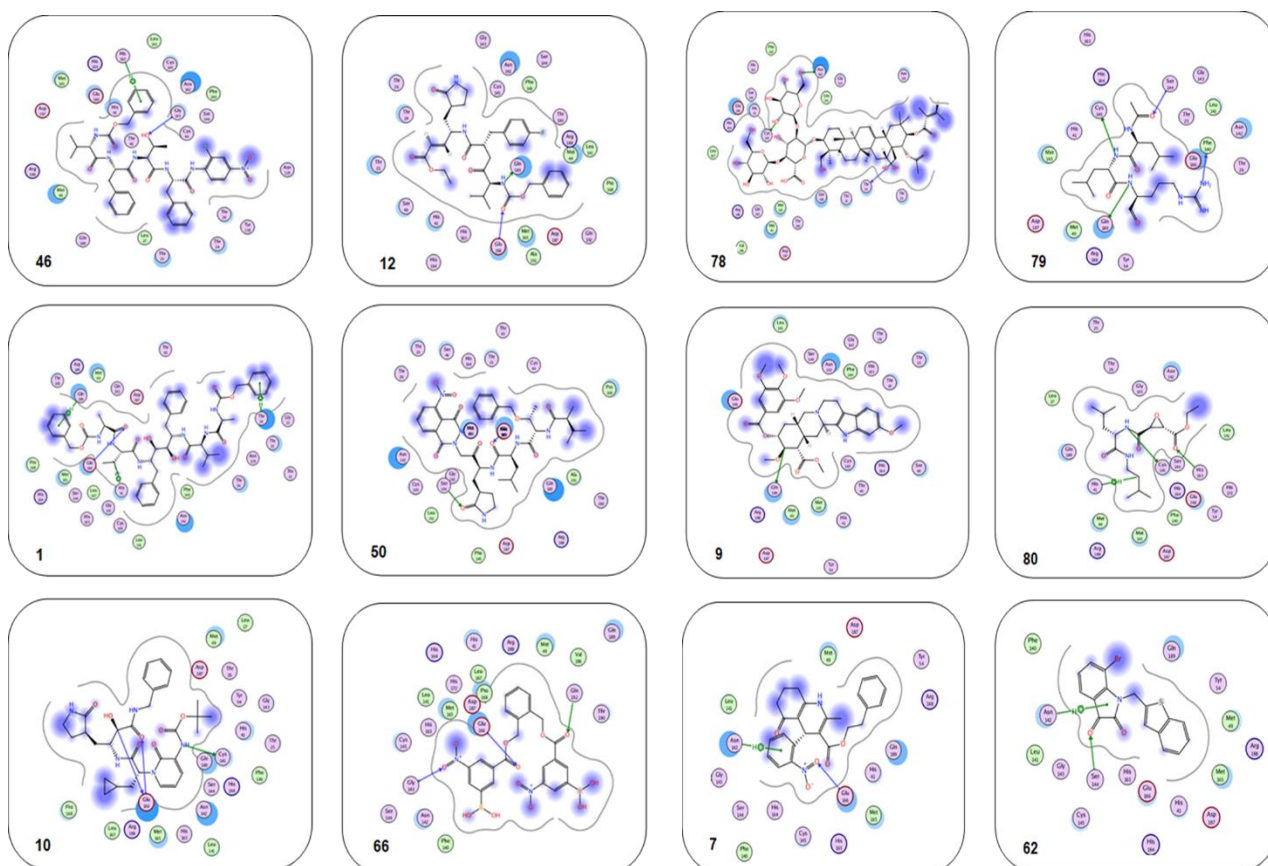
Figure 2. D images of CoV-2 3CL^{Pro} amino acid interactions with Tetrapeptide anilide, α, β-Unsaturated ester, TL-3, Ketoglutamine, α-ketoamide, Aryl Boronic, Aescin, Leupeptin, Reserpine, Loxistatin, MP576 and Isatin

Conclusion

Main proteinase is an intriguing target for inhibiting the viral reproduction cycle and treating infection with COVID-19. The goal of this work was to use in silico techniques to analyse the antiviral ability of a set of previously known inhibitors against 3CL^{Pro} of coronavirus. The 3CL^{Pro} of coronaviruses may be significantly inhibited by these inhibitors. Between the studied 80 compounds, compounds number 7, 9, 10, 12, 50, 62, 66, 79, and 80 showed binding interactions higher than those of 3CL^{Pro} of CoV-1 and/or MERS-CoV and successfully avoided detection during drug-likeness tests. These findings imply that we have explored good hits nominee for the improvement of therapeutic medicines against COVID-19. Animal investigations and proper clinical trials will eventually be required to prove the possible preventative and therapeutic impact of these substances.

Acknowledgment

Author's Declaration

- Conflicts of Interest: None.
- We hereby confirm that all the Figures and Tables in the manuscript are ours. Furthermore, any Figures and images, that are not ours, have been included with the necessary permission for re-publication, which is attached to the manuscript.
- Ethical Clearance: The project was approved by the local ethical committee at University of Mosul

Authors' Contribution

T. W. J. has contributed in drafting the manuscript, conception revision and proofreading. W. J. and M. A. Q. have contributed in conceptualization, methodology, investigation, and supervision. T. W. J., M. A. Q. and H.Y. H. have contributed in validation, resources and data curation. T. W J. , M. A Q., H.Y. H. and G. Q. I. have contributed in project administration.

References

1. Shereen MA, Khan S, Kazmi A, Bashir N, Siddique R. COVID-19 infection: Emergence, transmission, and characteristics of human coronaviruses. J Adv Res. 2020; 24: 91-98.https://doi.org/10.1016/j.jare.2020.03.005
2. Rothan HA, Byrareddy SN. The epidemiology and pathogenesis of coronavirus disease (COVID-19) outbreak. J Autoimmun. 2020; 109: 102433. https://doi.org/10.1016/j.jaut.2020.102433
3. Ye ZW, Yuan S, Yuen KS, Fung SY, Chan CP, Jin DY. Zoonotic origins of human coronaviruses. Int J Biol Sci. 2020; 16 (1): 1686-1697. https://doi.org/10.7150/ijbs.45472
4. Sabbah DA, Hajjo R, Bardaweel SK, Zhong HA. An updated review on betacoronavirus viral entry inhibitors: learning from past discoveries to advance COVID-19 drug discovery. Curr Top Med Chem. 2021; 21 (7): 571-596. https://doi.org/10.2174/1568026621666210119111409
5. Shirato K, Melaku SK, Kawachi K, Nao N, Iwata-Yoshikawa N, Kawase M, et al. Middle East respiratory syndrome coronavirus in dromedaries in Ethiopia is antigenically different from the Middle East isolate EMC Front Microbiol. 2019; 10: 1326.https://doi.org/10.3389/fmicb.2019.01326
6. Mann R, Perisetti A, Gajendran M, Gandhi Z, Umapathy C, Goyal H. Clinical characteristics, diagnosis, and treatment of major coronavirus outbreaks. Front Med. 2020; 7: 581521. https://doi.org/10.3389/fmed.2020.581521
7. Organization WH. Naming the coronavirus disease (COVID-19) and the virus that causes it. Braz J Implantol Health Sci. 2020; 2(3): 2020. https://bjihs.emnuvens.com.br/bjihs/article/view/173
8. Devi S, Raj A, Kumar P. Corona Virus: A detail Study on Covid-19. Covid 19: Impact and Response

Volume II. 1st ed. Maharashtra India: Bhumi Publishing; 2021. 53p.

9. Chan JF-W, Kok K-H, Zhu Z, Chu H, To KK-W, Yuan S, et al. Genomic characterization of the 2019 novel human-pathogenic coronavirus isolated from a patient with atypical pneumonia after visiting Wuhan. Emerg. microbes infect. 2020; 9 (1): 221-236.https://doi.org/10.1080/22221751.2020.1719902

10. Prajapat M, Sarma P, Shekhar N, Avti P, Sinha S, Kaur H, et al. Drug targets for corona virus: A systematic review. Indian J Pharmacol. 2020; 52(1): 56-65. https://doi.org/10.4103/ijp.IJP_115_20

11. Tsai PH, Wang ML, Yang DM, Liang KH, Chou SJ, Chiou SH, et al. Genomic variance of Open Reading Frames (ORFs) and Spike protein in severe acute respiratory syndrome coronavirus 2 (SARS-CoV-2). J Chin Med Assoc 2020; 83 (8): 725-732.https://doi.org/10.1097/JCMA.0000000000000387

12. Uzunian A. Coronavirus SARS-CoV-2 and Covid-19. J Bras Patol Med Lab. 2020; 56: 1-14. https://doi.org/10.5935/1676-2444.20200053

13. Ng CS, Stobart CC, Luo H. Innate immune evasion mediated by picornaviral 3C protease: Possible lessons for coronaviral 3C-like protease?. Rev Med Virol. 2021; 31 (5): 1-22. https://doi.org/10.1002/rmv.2206

14. Jeske L, Placzek S, Schomburg I, Chang A, Schomburg D. BRENDA in 2019: a European ELIXIR core data resource. Nucleic Acids Res. 2019; 47 (D1): D542-D549.https://doi.org/10.1093/nar/gky1048

15. Zhang L, Lin D, Sun X, Curth U, Drosten C, Sauerhering L, et al. Crystal structure of SARS-CoV-2 main protease provides a basis for design of improved α-ketoamide inhibitors. Sci. 2020; 368 (6489): 409-412. https://doi.org/10.1126/science.abb3405

16. Ullrich S, Nitsche C. SARS-CoV-2 Papain-Like Protease: Structure, Function and Inhibition. Chem Bio Chem 2022; 23 (19): e202200327.https://doi.org/10.1002/cbic.202200327

17. Qiu Y, Xu K. Functional studies of the coronavirus nonstructural proteins. STE Medicine 2020; 1 (2): e39-e39. https://doi.org/10.37175/stemedicine.v1i2.39

18. Wang KY, Liu F, Jiang R, Yang X, You T, Liu X, et al. Structure of Mpro from COVID-19 virus and discovery of its inhibitors. Nature. 2020; 582 (7811): 289-93. https://doi.org/10.1101/2020.02.26.964882

19. Wang M, Cao R, Zhang L, Yang X, Liu J, Xu M, et al. Remdesivir and chloroquine effectively inhibit the recently emerged novel coronavirus (2019-nCoV) in vitro. Cell Res. 2020; 30 (3): 269-271. https://doi.org/10.1038/ s41422-020-0282-0

20. Lai C-C, Shih T-P, Ko W-C, Tang H-J, Hsueh P-R. Severe acute respiratory syndrome coronavirus 2 (SARS-CoV-2) and coronavirus disease-2019 (COVID-19): The epidemic and the challenges. Int J Antimicrob Agents. 2020; 55 (3): 105924. https://doi.org/10.1016/j.ijantimicag.2020.105924

21. Morse JS, Lalonde T, Xu S, Liu WR. Learning from the past: possible urgent prevention and treatment options for severe acute respiratory infections caused by 2019-nCoV. Chem biochem. 2020; 21 (5): 730-738. https://doi.org/10.1002/cbic.202000047

22. Lu H. Drug treatment options for the 2019-new coronavirus (2019-nCoV). Bio Science Trends. 2020; 14 (1): 69-71. https://doi.org/10.5582/bst.2020.01020

23. Elfiky AA. Natural products may interfere with SARS-CoV-2 attachment to the host cell. J Biomol Struct Dyn. 2021; 39 (9): 3194-3203. https://doi.org/10.1080/07391102.2020.1761881

24. Atanasov AG, Zotchev SB, Dirsch VM, Supuran CT. Natural products in drug discovery: advances and opportunities. Nat Rev Drug Discov. 2021; 20 (3): 200-216. https://doi.org/10.1038/ s41573-020-00114-z

25. Al-Karmalawy AA, Khattab M. Molecular modelling of mebendazole polymorphs as a potential colchicine binding site inhibitor. New J Chem. 2020; 44 (33): 13990-13996. https://doi.org/10.1039/d0nj02844d

26. Ghanem A, Emara HA, Muawia S, Abd El Maksoud AI, Al-Karmalawy AA, Elshal MF. Tanshinone IIA synergistically enhances the antitumor activity of doxorubicin by interfering with the PI3K/AKT/mTOR pathway and inhibition of topoisomerase II: in vitro and molecular docking studies. New J Chem. 2020; 44 (40): 17374-17381. https://doi.org/10.1039/d0nj04088f

27. Hussen NH. Synthesis, characterization, molecular docking, ADMET prediction, and anti-inflammatory activity of some Schiff bases derived from salicylaldehyde as a potential cyclooxygenase inhibitor. Baghdad Sci J. 2023. https://dx.doi.org/10.21123/bsj.2023.7181

28. Chang CC, Hsu HJ, Wu TY, Liou JW. Computer-aided discovery, design, and investigation of COVID-19 therapeutics. Tzu Chi Med J. 2022; 34 (3): 276-286. https://doi.org/10.4103/tcmj.tcmj_318_21

29. 29. Ibrahim AA. A Theoretical Study of the Docking of Medicines with some Proteins. Baghdad Sci J. 2023; 20 (2): 0319-0319. http://dx.doi.org/10.21123/bsj.2022.7064

30. Majumdar S, Nandi SK, Ghosal S, Ghosh B, Mallik W, Roy ND, et al. Deep learning-based potential ligand prediction framework for COVID-19 with

drug–target interaction model. Cognit Comput. 2021; 1-13. https://doi.org/10.1007/s12559-021-09840-x

31. Wu C-Y, Jan J-T, Ma S-H, Kuo C-J, Juan H-F, Cheng Y-SE, et al. Small molecules targeting severe acute respiratory syndrome human coronavirus. Proc Natl Acad Sci. 2004; 101 (27): 10012-10017. https://doi.org/10.1073/pnas.0403596101

32. Blanchard JE, Elowe NH, Huitema C, Fortin PD, Cechetto JD, Eltis LD, et al. High-throughput screening identifies inhibitors of the SARS coronavirus main proteinase. Chem Biol. 2004; 11 (10): 1445-1453. https://doi.org/10.1016/j.chembiol.2004.08.011

33. Kao RY, Tsui WH, Lee TS, Tanner JA, Watt RM, Huang J-D, et al. Identification of novel small-molecule inhibitors of severe acute respiratory syndrome-associated coronavirus by chemical genetics. Chem Biol. 2004; 11 (9): 1293-1299.https://doi.org/10.1016/j.chembiol.2004.07.013

34. Hsu JT-A, Kuo C-J, Hsieh H-P, Wang Y-C, Huang K-K, Lin CP-C, et al. Evaluation of metal-conjugated compounds as inhibitors of 3CL protease of SARS-CoV. FEBS lett. 2004; 574 (1-3): 116-120. https://doi.org/10.1016/j.febslet.2004.08.015

35. Shie J-J, Fang J-M, Kuo T-H, Kuo C-J, Liang P-H, Huang H-J, et al. Inhibition of the severe acute respiratory syndrome 3CL protease by peptidomimetic α, β-unsaturated esters. Bioorg Med Chem. 2005; 13 (17): 5240-5252. https://doi.org/10.1016/j.bmc.2005.05.065

36. Shie J-J, Fang J-M, Kuo C-J, Kuo T-H, Liang P-H, Huang H-J, et al. Discovery of potent anilide inhibitors against the severe acute respiratory syndrome 3CL protease. J Med Chem. 2005; 48 (13): 4469-4473. https://doi.org/10.1021/jm050184y

37. Jain RP, Pettersson HI, Zhang J, Aull KD, Fortin PD, Huitema C, et al. Synthesis and evaluation of keto-glutamine analogues as potent inhibitors of severe acute respiratory syndrome 3CLpro. J Med Chem. 2004; 47 (25): 6113-6116. https://doi.org/10.1021/jm0494873

38. Chen L-R, Wang Y-C, Lin YW, Chou S-Y, Chen S-F, Liu LT, et al. Synthesis and evaluation of isatin derivatives as effective SARS coronavirus 3CL protease inhibitors. Bioorg Med Chem Lett. 2005; 15 (12): 3058-3062. https://doi.org/10.1016/j.bmcl.2005.04.027

39. Bacha U, Barrila J, Velazquez-Campoy A, Leavitt SA, Freire E. Identification of novel inhibitors of the SARS coronavirus main protease 3CLpro. Biochem. 2004; 43 (17): 4906-4912. https://doi.org/10.1021/bi0361766

40. Kim JW, Cho H, Kim E, Shim SH, Yang J-L, Oh WK. Antiviral escin derivatives from the seeds of Aesculus turbinata Blume (Japanese horse chestnut). Bioorg Med Chem Lett. 2017; 27 (13): 3019-3025. https://doi.org/10.1016/j.bmcl.2017.05.022.

41. Fu L, Shao S, Feng Y, Ye F, Sun X, Wang Q, et al. Mechanism of microbial metabolite leupeptin in the treatment of COVID-19 by traditional chinese medicine herbs. ASM Journals. Mbio. 2021; 12 (5): e02220-21 https://doi.org/10.1128/mBio.02220-21

Baghdad Science Journal

مقارنة دراسة نظرية لمثبطات انزيم البروتينيز لانواع مختلفة من الفيروسات التاجية

تهاني وليد جهاد، هيفاء يونس حسين، محمد عدنان محمد، غسان قاسم اسماعيل

قسم الكيمياء، كلية العلوم، جامعة الموصل، موصل، العراق.

الخلاصة

فيروسات كورونا تضم فيروسات الحمض النووي الريبي الموجبة مع نتوءات بروتينية شوكية تسمح للفيروس بالاختراق والتأثير على الخلايا المضيفة. ان ظهور فيروس كورونا المتلازمة التنفسية الحادة الوخيمة (SARS-CoV) ومتلازمة الشرق الأوسط التنفسية التاجية (MERS-CoV) ، كأمراض مميتة بفيروس كورونا البشري، مم اثار اهتمامًا كبيرًا في المجتمع الطبي. ان التفشي السريع والعالمي لفيروس كورونا البشري الجديد الناتج عن سلالة جديدة من الفيروس التاجي 2 (CoV-2) ادى إلى تعزيز الحاجة لايجاد علاج فعال لـCOVID-19. ان انزيم M^{Pro} برز كهدف علاجي جذاب لفيروسات كورونا، وهو المسؤول عن النسخ والنسخ المتماثلة لفيروسات كورونا. ان تشخيص ادوية محتملة هي حاجة ملحة وحاسمة للمجتمع الطبي. تم استخدام الالتحام الجزيئي استعمل لوصف انزيم البروتيز وتقييم قدرة العديد من مثبطات انزيم M^{Pro} الطبيعية المعروفة والمختبرة مختبريا. تم اختيار ستة وسبعين مركبًا طبيعيًا ذو فعالية مثبطة معروفة وأربعة أدوية مختبرة ضد CoV-1 اختيرت في دراسة الالتحام الجزيئي. كشفت دراساتنا النظرية أن العديد من هذه الجزيئات تظهر الفة ارتباط عالية للعديد من انزيمات CoV-2 ومقارنة المفضلة منها مع انزيمات CoV-1 و MERS. يشير بحثنا إلى أن هذه الجزيئات يمكن أن تكون مثبطة لانزيم CoV-2 M^{Pro}. مما يدل على إمكانية إعادة توصيفها كمركبات مضادة للفيروسات على نطاق واسع.

الكلمات المفتاحية: كوفيد-19، سستين بروتيز، انزيم البروتينيز، الالتحام الجزيئي، المركبات الطبيعية.